Original Article

pISSN 2234-7518 • eISSN 2005-372X
https://doi.org/10.4041/kjod.2019.49.5.326

THE KOREAN JOURNAL of ORTHODONTICS
KJO

Application of the foramina of the trigeminal nerve as landmarks for analysis of craniofacial morphology

Ba-Da Lim
Dong-Soon Choi
Insan Jang
Bong-Kuen Cha

Department of Orthodontics, College of Dentistry, Gangneung-Wonju National University, Gangneung, Korea

Objective: The objective of this study was to develop new parameters based on the foramina of the trigeminal nerve and to compare them with the conventional cephalometric parameters in different facial skeletal types. **Methods:** Cone-beam computed tomography (CBCT) scans and cephalograms from 147 adult patients (57 males and 90 females; mean age, 26.1 years) were categorized as Class I ($1^{\circ} < ANB < 3^{\circ}$), Class II ($ANB > 5^{\circ}$), and Class III ($ANB < -1^{\circ}$). Seven foramina in the craniofacial area—foramen rotundum (Rot), foramen ovale (Ov), infraorbital foramen, greater palatine foramen, incisive foramen (IF), mandibular foramen (MDF), and mental foramen (MTF)—were identified in the CBCT images. Various linear, angular, and ratio parameters were compared between the groups by using the foramina, and the relationship between the new parameters and the conventional cephalometric parameters was assessed. **Results:** The distances between the foramina in the cranial base did not differ among the three groups. However, the Rot-IF length was shorter in female Class III patients, while the Ov-MTF length, MDF-MTF length, and Ov-MDF length were shorter in Class II patients than in Class III patients of both sexes. The MDF-MTF/FH plane angle was larger in Class II patients than in Class III patients of both sexes. Most parameters showed moderate to high correlations, but the Ov-MDF-MTF angle showed a relatively low correlation with the gonial angle. **Conclusions:** The foramina of the trigeminal nerve can be used to supplement assessments based on the conventional skeletal landmarks on CBCT images.
[Korean J Orthod 2019;49(5):326-337]

Key words: Computed tomography, Anatomy, Foramen, Trigeminal nerve

Received January 7, 2019; Revised June 19, 2019; Accepted June 22, 2019.

Corresponding author: Dong-Soon Choi.
Professor, Department of Orthodontics, College of Dentistry, Gangneung-Wonju National University, 7 Jukheon-gil, Gangneung 25457, Korea.
Tel +82-33-640-3152 **e-mail** dschoi@gwnu.ac.kr

How to cite this article: Lim BD, Choi DS, Jang I, Cha BK. Application of the foramina of the trigeminal nerve as landmarks for analysis of craniofacial morphology. Korean J Orthod 2019;49:326-337.

INTRODUCTION

Cephalometric radiographs were introduced in the 1940s, and they allowed analysis of malocclusion via measurement of the hard tissues of the craniofacial region.[1-5] Although cephalometric radiography has numerous advantages, it also has inherent limitations imposed by image enlargement, the two-dimensional (2D) nature of the scans, and the overlapping of structures.[6-8] Most landmarks used in cephalometric analysis, such as A point, B point, pogonion, menton, and gonion, are artificial landmarks that are defined geometrically on the outline of the bone, probably to ease of identification.

With the introduction of three-dimensional (3D) cone-beam computed tomography (CBCT), anatomical structures such as the craniofacial foramen are now being used as landmarks for craniofacial analysis,[9-13] with high reliability and accuracy.[11,12] Cutright et al.[13] reported small but significant differences in the position of the infraorbital foramen (IOF) and the mental foramen (MTF) between Caucasian and African-American individuals and males and females. Some authors have used the mandibular foramen (MDF) and the MTF to analyze the mandibular morphology.[9,10]

In general, the growth of the brain and nerve tissues accelerates earlier than that of other tissues or organs like the tonsils, adenoids, muscles, skeleton, and genital organs, and bone structures adjacent to nerve tissues adhere to the neural pattern of growth.[14] This is the reason why the cranial base is used as a superimposing area for craniofacial analysis. Since the foramen is a biological structure made for a nerve to pass through, it can be inferred that the foramen stabilizes earlier than other areas. In 1969, an implant study by Björk[15] showed that the mandibular canal was relatively stable during the growth period, whereas marked bone resorption or apposition were observed on the gonial angle, below the symphysis, and on the condylar process. Recently, Captier et al.[9] reported that the length of the mandibular canal (from the MDF to the MTF) was symmetric, while those of the ramus, condylar process, and mandibular notch were asymmetric, suggesting that the neural part of the mandible is more stable than the muscular part, which may show variations to adapt to the masticatory apparatus.

The trigeminal nerve is divided into three branches—the ophthalmic nerve, the maxillary nerve, and the mandibular nerve—and is widely distributed over the maxillomandibular region. As a result, there are many foramina for the trigeminal nerve in the cranial base, the maxilla, and the mandible. A few reports have used these foramina for craniofacial analysis in patients with different skeletal facial types.[9,10,13] The aims of this study were to (1) develop parameters based on the craniofacial foramina on CBCT images, (2) determine whether there are any significant differences in these parameters among Class I, Class II, and Class III malocclusion groups, and (3) establish the relationship between these parameters and the conventional cephalometric parameters. The null hypothesis of this study was that the parameters based on the foramina of the trigeminal nerve showed no differences in different facial skeletal types and showed no relationship with conventional cephalometric parameters.

MATERIALS AND METHODS

Samples

The samples were collected from the archive of patients who visited the Department of Orthodontics, Gangneung-Wonju National University Dental Hospital between December 2014 and January 2017. Inclusion criteria were (1) age over 18 years, (2) no craniofacial anomalies, (3) no facial asymmetry, (4) no history of orthodontic treatment, and (5) availability of cephalometric radiographs and CBCT scans including the cranial base. Patients with an A point-nasion-B point (ANB) angle of 1 to 3° were enrolled in the Class I group, those with an ANB angle of 5° or more were enrolled in the Class II group, and those with an ANB angle of −1° or less were enrolled in the Class III group. A total of 147 patients (57 males and 90 females; mean age, 26.1 years) were included in this study (Table 1). This study was approved by the Institutional Review Board of the Gangneung-Wonju National University Dental Hospital (IRB No. 2016-018).

Cephalometric analysis

Cephalometric radiographs used in this study were

Table 1. Mean and standard deviation of age and ANB angle in the three groups

Group	Male (N = 57)			Female (N = 90)		
	Number	Age (yr)	ANB (°)	Number	Age (yr)	ANB (°)
Class I	29	25.5 ± 7.5	2.1 ± 0.6	37	25.5 ± 8.4	2.2 ± 0.6
Class II	11	26.0 ± 8.4	6.3 ± 1.0	40	27.7 ± 10.3	6.8 ± 1.3
Class III	17	27.5 ± 9.1	−2.7 ± 1.5	13	22.3 ± 5.1	−2.8 ± 1.9

ANB, A point-nasion-B point angle; Class I, 1° < ANB < 3°; Class II, ANB > 5°, Class III, ANB < −1°.

 https://doi.org/10.4041/kjod.2019.49.5.326

obtained using CX-90SP (Asahi Roentgen Ind., Kyoto, Japan) in the patients' habitual occlusion. Six angular and seven linear parameters were measured using Quick Ceph Studio software (Quick Ceph Systems, San Diego, CA, USA). The magnification ratio of the radiographs (110%) was not calibrated in the present study.

Cone-beam computed tomography analysis

The CBCT scans used in this study were taken using Alphard-3030 (Asahi Roentgen Ind.) with a field of view of 200 × 179 mm and voxel size of 0.39 mm. 3D analysis of CBCT images was performed using OnDemand software (Cybermed, Seoul, Korea). Each CBCT image was oriented with three reference planes and three axes, and the origin (0, 0, 0) was set at the sella (Figure 1). The horizontal plane was parallel to the Frankfort horizontal (FH) plane, which consisted of the right porion and bilateral orbitales. The coronal and sagittal planes were perpendicular to each other and to the horizontal plane.

This study analyzed the foramina for the trigeminal nerve, which distributes into the maxilla and the mandible. Briefly, the maxillary nerve leaves the skull through the foramen rotundum (Rot), then distributes to the midface for sensation from the maxilla, nasal cavity, sinuses, and the palate. The infraorbital nerve, a branch of the maxillary nerve, emerges on the face through the IOF, and the greater palatine nerve and the incisive nerve emerge on the hard palate through the greater palatine foramen (GPF) and incisive foramen (IF), respectively. The mandibular nerve exits the cranial cavity through the foramen ovale (Ov), then distributes to the mandible through many branches. The inferior alveolar nerve, a branch of the mandibular nerve, enters the MDF and exits through the MTF.[16,17] In this study, seven landmarks—Rot, Ov, IOF, GPF, IF, MDF, and MTF—were identified three-dimensionally on CBCT images (Figure 2). The definitions for landmark identification are summarized in Table 2. To determine the method errors in landmark identification, ten CBCT images were randomly selected and the locations were evaluated by one examiner (B.D.L.) with a one-week interval. The method errors calculated by Dahlberg formula[18] were less than 0.5 mm. Various linear, angular, and ratio parameters were created using the above anatomical landmarks (Figure 3). The average values were used in the case of bilateral measurements.

Statistical analysis

Since the Shapiro–Wilk test showed that the measurements did not follow a normal distribution ($p > 0.05$), a nonparametric test was used. The Kruskal–Wallis test was performed to assess for significant differences among the three groups. In addition, differences between two groups were examined using the Mann–Whitney *U* test. Statistical significance was established at $p < 0.05$, and Bonferroni correction was used to adjust the significance levels for the differences between two groups ($p < 0.016$). Some cephalometric parameters and CBCT parameters were selected for Spearman's correlation test, which assessed the relationship between the conventional cephalometric parameters and new CBCT parameters. Statistical analyses were performed using SPSS (ver. 18.0; SPSS Inc., Chicago, IL, USA).

RESULTS

Tables 3 and 4 show comparison of the conventional cephalometric parameters among three groups in each sex. Briefly, the length of the S-N line measured at the cranial base showed no difference among groups, but the length of Co-A in female patients was shorter in Class III than in Class II cases ($p = 0.013$), while the

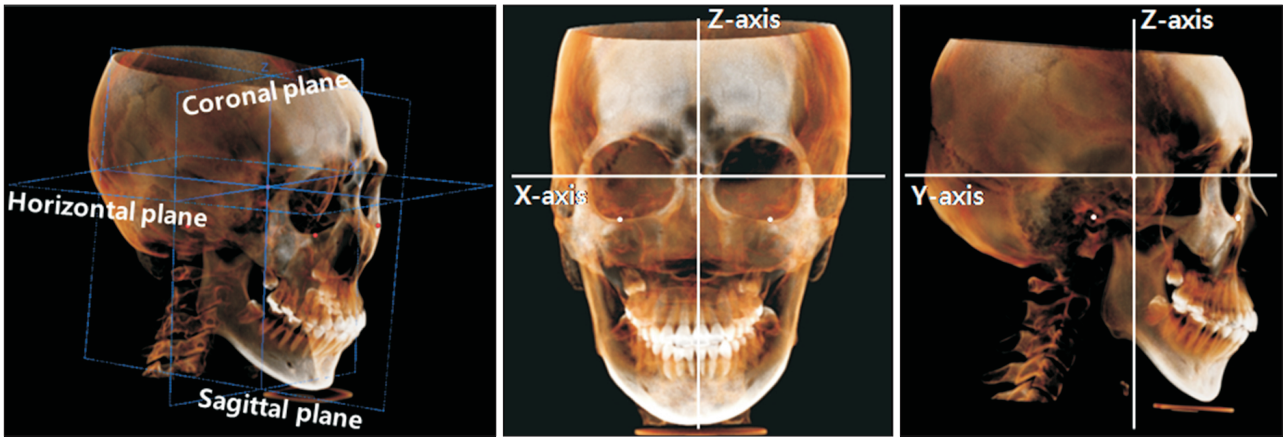

Figure 1. Three-dimensional reconstruction and orientation of the cone-beam computed tomography image with three reference planes and three axes. The origin was set at the sella.

https://doi.org/10.4041/kjod.2019.49.5.326

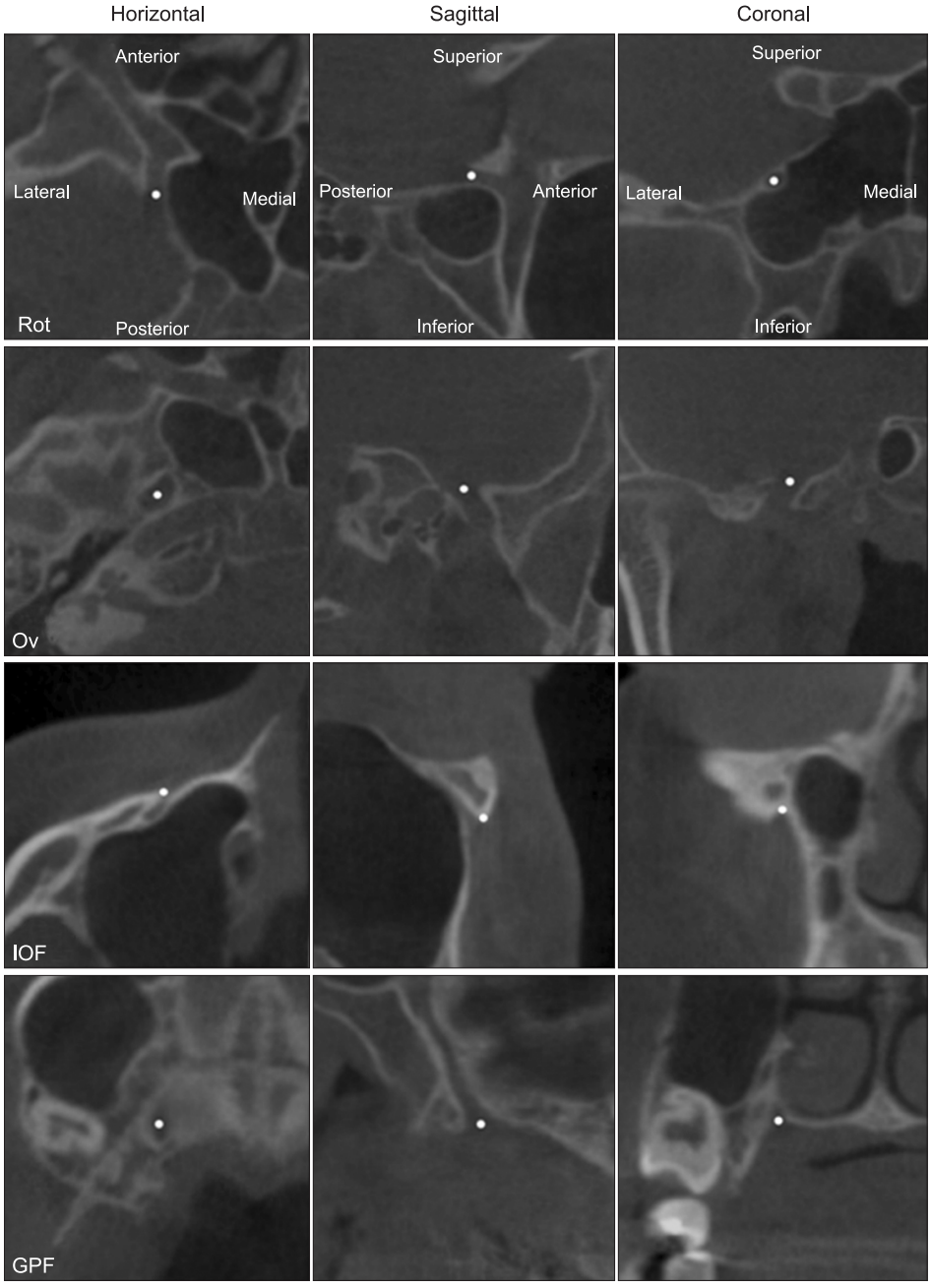

Figure 2. Description of landmarks in cone-beam computed tomography images. The images in each column have the same orientation as the corresponding images in the first row.
Rot, Foramen rotundum; Ov, foramen ovale; IOF, infraorbital foramen; GPF, greater palatine foramen; IF, incisive foramen; MDF, mandibular foramen; MTF, mental foramen.

length of Co-Pog in both genders was longer in Class III than in Class II cases ($p < 0.01$). There were also differences in vertical relation. Females in the Class II group showed shorter S-Go length and longer ANS-Me length and a larger Go-Me to FH plane angle, in comparison to those in the Class I group ($p < 0.05$).

Table 5 shows the results of group differences of the new parameters using the foramina in male. In the linear measurements, Ov-MTF, MDF-MTF, and Ov-MDF were shorter in the Class II (88.3 mm, 55.3 mm, and 44.9 mm, respectively) than in the Class III group (98.0 mm, 59.0 mm, and 50.7 mm, respectively) ($p < 0.05$). In the angular measurements, Ov-MDF to FH plane angle, Ov-MTF to FH plane angle, and MDF-MTF to FH plane angle were smaller in Class III (63.4°, 51.4°, and 31.9°, respectively) than in Class I (66.3°, 55.3°, and 35.0°, respectively) and Class II (66.6°, 56.2°, and 36.0°, respectively) patients ($p < 0.01$). The Rot-GPF/Ov-MDF ratio was significantly higher in Class II (0.82) than in Class I (0.77) and Class III (0.72) patients ($p < 0.01$). The Rot-IF/Ov-MTF ratio was the highest in Class II (0.77) patients, followed by the Class I (0.70) and Class III groups (0.67) ($p < 0.001$).

The differences between female groups shown in Ta-

 https://doi.org/10.4041/kjod.2019.49.5.326

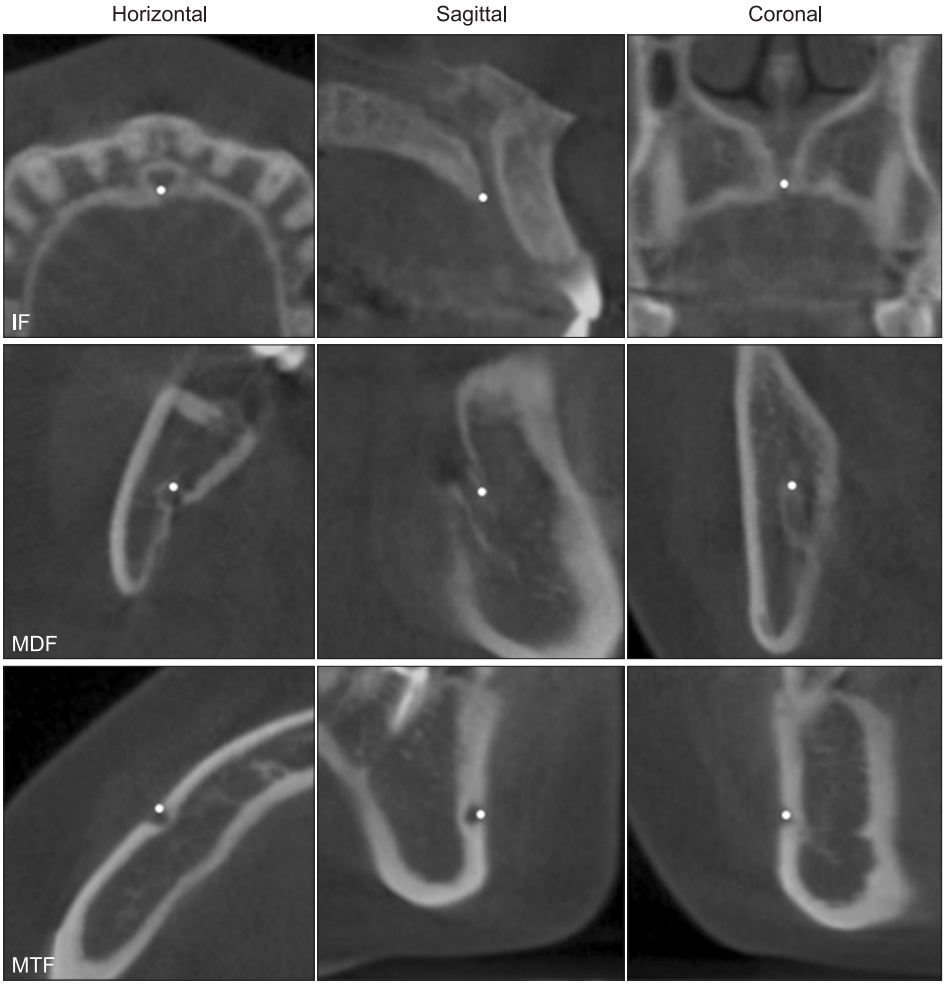

Figure 2. Continued.

ble 6 were generally similar to those in the male groups. Ov-MTF, MDF-MTF, and Ov-MDF lengths were shorter in Class II than in the other groups ($p < 0.01$). Ov-MDF to FH plane angle, Ov-MTF to FH plane angle, and MDF-MTF to FH plane angle were also smaller in Class III than in the other groups ($p < 0.01$). The Rot-GPF/Ov-MDF ratio and the Rot-IF/Ov-MTF ratio were higher in the Class II group than in the Class III group ($p < 0.001$). Additionally, some parameters showed significant differences in female groups. The Rot-IF length was shorter in the Class III female group (58.7 mm) than in the Class I (62.6 mm) and Class II (62.2 mm) female groups ($p = 0.01$). The GPF-IF/MDF-MTF and Rot-IOF/MDF-MTF ratios were significantly larger in Class II (0.68, 0.92, respectively) than in Class I (0.64, 0.86, respectively) ($p < 0.01$).

Figure 4 describes the results of Spearman correlation analysis between conventional cephalometric parameters and the new foramina-based CBCT parameters. There were moderate to high correlations between both parameters. Specifically, there was a high correlation between the mandibular length (Co-Pog) and Ov-MTF length ($r = 0.895$, $p < 0.001$) and between the anterior facial height (N-Me) and IOF-MTF length ($r = 0.899$, $p < 0.001$). Among the angular parameters, the mandibular plane angle (Go-Me to FH plane) showed a high correlation with MDF-MTF to FH plane angle ($r = 0.716$, $p < 0.001$); however, there was a relatively low correlation between the palatal plane angle (ANS-PNS to FH plane) and GPF-IF to FH plane angle ($r = 0.417$, $p < 0.001$) and between the gonial angle (Ar-Go-Me) and Ov-MDF-MTF angle ($r = 0.345$, $p < 0.001$). Description of the variables used in this study are depicted in Table 3.

DISCUSSION

Between the 1970s and 1980s, the trigeminal nerve received great attention from orthodontic researchers in relation to facial growth and development.[19-24] Moss[21,22] suggested the neurotrophic effect on orofacial growth in which the neural center regulates the growth of the peripheral tissues through non-impulse transmitting neural function. The control exerted by the trigeminal nerve on maxillomandibular growth was hypothesized at

https://doi.org/10.4041/kjod.2019.49.5.326

Table 2. Definition of landmarks in cone-beam computed tomography analysis

Landmark	Abbreviation	Meaning	Definition
Foramen rotundum	Rot	Exit hole of maxillary branch (V2) of trigeminal nerve from the cranium	Center of the foramen
Foramen ovale	Ov	Exit hole of mandibular branch (V3) of trigeminal nerve from the cranium	Center of the foramen
Infraorbital foramen	IOF	Exterior end of the infraorbital canal and transmits the infraorbital nerve, a branch of maxillary nerve	The most superolateral point of the foramen
Greater palatine foramen	GPF	Exterior end of greater palatine canal and transmits the greater palatine nerve, a branch of maxillary nerve	Center of the foramen
Incisive foramen	IF	End of incisive canal and transmits the incisive nerve, a branch of maxillary nerve	The most posterior point of the foramen
Mandibular foramen	MDF	Opening on the internal surface of the ramus of the mandible and transmits mandibular nerve	The most anterosuperior point of the foramen outline
Mental foramen	MTF	Opening on the anterior surface of the mandible and transmits the terminal branches of the inferior alveolar nerve, a branch of mandibular nerve	The most anterior point of the foramen

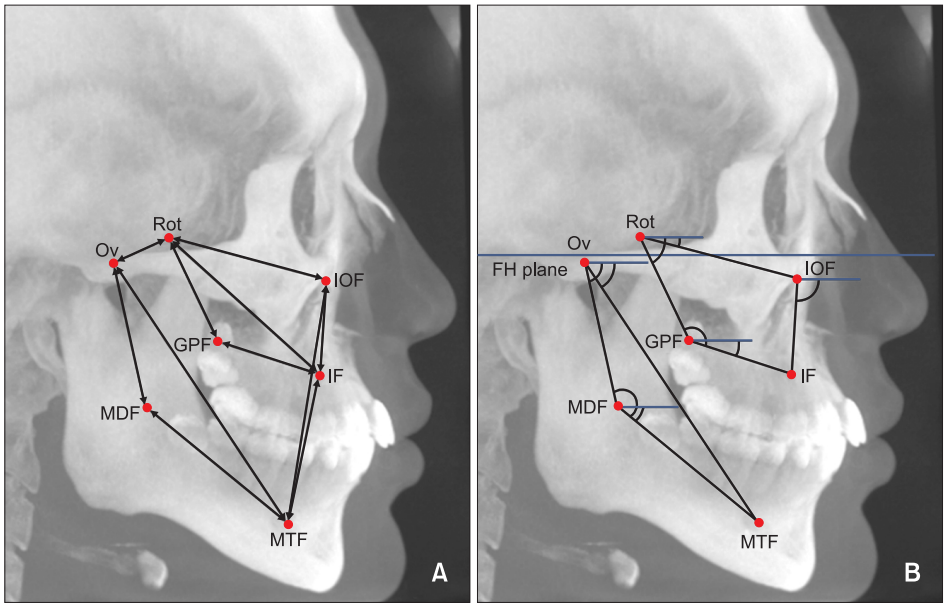

Figure 3. Linear **(A)** and angular **(B)** parameters in cone-beam computed tomography (CBCT) images. Identification of the landmark and measurements were performed three-dimensionally. To visualize the location of the landmarks and measurement parameters, they were simply drawn in the lateral maximum projection image of CBCT.
FH, Frankfort horizontal plane. See Table 2 for definition of each landmark.

that point, however it was not supported by later animal studies that evaluated the growth of craniofacial bone after resection of the trigeminal nerve.[19,23,24] The aim of this study is not to rekindle the old controversy regarding the potential regulating activity of the trigeminal nerve in facial growth. However, the cranium and the cranial base grow earlier than other facial structures to adapt to the early growth of the brain.[14] Therefore, we inferred that the craniofacial and maxillomandibular foramina through which the nerve passes may also show a neural pattern of growth, i.e., they may grow earlier than other areas of the bone. Therefore, the foramina may be more stable structures for craniofacial analysis, since Björk[15] reported that the mandibular canal was

 https://doi.org/10.4041/kjod.2019.49.5.326

Table 3. Comparison of cephalometric parameters between male patients in the three groups

Cephalometric parameter	Class I (n = 29)	Class II (n = 11)	Class III (n = 17)	Kruskal–Wallis	Mann–Whitney
Anterior cranial base length (S-N) (mm)	73.3 ± 2.9	73.1 ± 3.3	73.2 ± 3.3	0.999	
Maxillary length (Co-A) (mm)†	95.7 ± 5.1	98.1 ± 5.7	94.4 ± 4.6	0.078	
Mandibular length (Co-Pog) (mm)†	130.0 ± 6.5	123.5 ± 5.1	134.1 ± 5.0	< 0.001*	I, III > II
Mandibular body length (Go-Me) (mm)†	81.7 ± 5.0	80.7 ± 6.3	85.8 ± 4.3	0.014*	III > I
Posterior facial height (S-Go) (mm)†	97.7 ± 8.8	92.1 ± 5.9	96.8 ± 6.8	0.081	
Anterior facial height (N-Me) (mm)†	139.6 ± 5.6	137.4 ± 5.9	138.2 ± 5.3	0.801	
Lower anterior facial height (ANS-Me) (mm)†	78.2 ± 4.0	76.7 ± 4.8	76.9 ± 4.9	0.716	
SNA (°)	82.3 ± 4.3	82.6 ± 2.9	81.0 ± 3.5	0.322	
SNB (°)	80.2 ± 4.5	76.3 ± 3.0	83.6 ± 3.0	< 0.001*	III > II
ANB (°)	2.1 ± 0.6	6.3 ± 1.0	–2.7 ± 1.5	< 0.001*	II > I > III
Palatal plane angle (ANS-PNS/FH plane) (°)†	1.5 ± 2.2	0.7 ± 2.6	1.9 ± 3.4	0.744	
Mandibular plane angle (Go-Me/FH plane) (°)†	24.0 ± 3.6	26.5 ± 5.7	21.7 ± 5.9	0.335	
Gonial angle (Ar-Go-Me) (°)†	118.6 ± 6.3	116.9 ± 11.1	120.8 ± 9.1	0.138	

Values are presented as mean ± standard deviation.
S, Sella; N, nasion; Co, condylion; A, A point; Pog, pogonion; Go, gonion; Me, menton; ANS, anterior nasal spine; SNA, sella-nasion-A point; SNB, sella-nasion-B point; ANB, A point-nasion-B point; PNS, posterior nasal spine; FH, Frankfort horizontal; Ar, articulare.
*$p < 0.05$.
†Parameters used for correlation analysis with cone-beam computed tomography parameters.

Table 4. Comparison of cephalometric parameters between female patients in the three groups

Cephalometric parameter	Class I (n = 37)	Class II (n = 40)	Class III (n = 13)	Kruskal–Wallis	Mann–Whitney
Anterior cranial base length (S-N) (mm)	68.8 ± 3.1	68.6 ± 2.9	69.6 ± 3.4	0.657	
Maxillary length (Co-A) (mm)†	89.2 ± 3.9	90.2 ± 4.4	86.1 ± 3.8	0.013*	II > III
Mandibular length (Co-Pog) (mm)†	119.4 ± 4.7	115.4 ± 4.6	123.3 ± 5.7	< 0.001*	I, III > II
Mandibular body length (Go-Me) (mm)†	79.3 ± 4.2	74.5 ± 4.1	80.1 ± 4.1	< 0.001*	I, III > II
Posterior facial height (S-Go) (mm)†	84.2 ± 5.5	81.1 ± 6.4	82.1 ± 4.4	0.025*	I > II
Anterior facial height (N-Me) (mm)†	127.4 ± 5.8	130.3 ± 6.7	127.9 ± 8.7	0.119	
Lower anterior facial height (ANS-Me) (mm)†	71.0 ± 4.7	74.4 ± 6.0	72.1 ± 7.4	0.017*	I < II
SNA (°)	81.5 ± 3.8	81.7 ± 3.1	78.8 ± 3.6	0.064	
SNB (°)	79.3 ± 3.9	75.0 ± 3.4	81.5 ± 3.7	< 0.001*	I, III > II
ANB (°)	2.2 ± 0.6	6.8 ± 1.3	–2.8 ± 1.9	< 0.001*	II > I > III
Palatal plane angle (ANS-PNS/FH plane) (°)†	0.9 ± 3.0	1.2 ± 3.2	2.8 ± 4.8	0.494	
Mandibular plane angle (Go-Me/FH plane) (°)†	25.4 ± 5.8	31.5 ± 6.4	27.3 ± 6.6	< 0.001*	I < II
Gonial angle (Ar-Go-Me) (°)†	118.2 ± 5.8	121.0 ± 5.8	125.0 ± 9.3	0.008*	I < III

Values are presented as mean ± standard deviation.
See Table 3 for definition of each landmark or measurement.
*$p < 0.05$.
†Parameters used for correlation analysis with cone-beam computed tomography parameters.

https://doi.org/10.4041/kjod.2019.49.5.326

Table 5. Comparison of foramina-based cone-beam computed tomography (CBCT) parameters in male patients in the three groups

CBCT parameter	Class I (n=29)	Class II (n=11)	Class III (n=17)	Kruskal-Wallis	Mann-Whitney
Rot-Ov (mm)	17.4 ± 1.8	17.7 ± 1.8	17.0 ± 1.6	0.743	
Rot-IOF (mm)	49.2 ± 3.3	47.1 ± 3.2	48.0 ± 3.4	0.186	
Rot-GPF (mm)	38.2 ± 4.3	36.9 ± 3.4	36.6 ± 3.8	0.454	
Rot-IF (mm)†	67.5 ± 5.3	67.8 ± 4.9	65.3 ± 3.5	0.228	
GPF-IF (mm)	35.7 ± 2.7	33.7 ± 2.8	35.2 ± 2.6	0.167	
IOF-IF (mm)	41.5 ± 3.0	42.4 ± 3.0	41.3 ± 1.9	0.716	
Ov-MTF (mm)†	96.2 ± 6.5	88.3 ± 5.3	98.0 ± 4.2	0.001*	I, III > II
MDF-MTF (mm)†	58.1 ± 3.8	55.3 ± 3.2	59.0 ± 2.9	0.022*	III > II
Ov-MDF (mm)†	49.9 ± 5.0	44.9 ± 3.6	50.7 ± 4.1	0.003*	I, III > II
IOF-MTF (mm)†	73.0 ± 4.1	69.5 ± 4.1	72.3 ± 4.6	0.083	
IF-MTF (mm)†	48.1 ± 2.7	45.8 ± 2.9	47.6 ± 4.2	0.108	
Rot-IOF to FH plane (°)	16.4 ± 4.3	15.9 ± 2.5	13.7 ± 2.9	0.076	
Rot-GPF to FH plane (°)	64.5 ± 4.0	63.3 ± 3.4	62.8 ± 3.3	0.244	
GPF-IF to FH plane (°)†	17.2 ± 4.0	18.2 ± 2.9	17.8 ± 2.9	0.669	
IOF-IF to FH plane (°)	48.6 ± 3.3	47.9 ± 2.9	50.0 ± 2.3	0.233	
Ov-MDF to FH plane (°)	66.3 ± 2.4	66.6 ± 3.8	63.4 ± 2.9	0.002*	I, II > III
Ov-MTF to FH plane (°)	55.3 ± 3.1	56.2 ± 2.8	51.4 ± 3.0	0.001*	I, II > III
MDF-MTF to FH plane (°)†	35.0 ± 3.1	36.0 ± 3.2	31.9 ± 4.0	0.008*	I, II > III
Ov-MDF-MTF angle (°)†	125.6 ± 3.4	123.4 ± 3.7	126.4 ± 3.9	0.110	
Rot-GPF/Ov-MDF	0.77 ± 0.06	0.82 ± 0.07	0.72 ± 0.06	0.001*	II > I, III
Rot-IF/Ov-MTF	0.70 ± 0.03	0.77 ± 0.04	0.67 ± 0.03	< 0.001*	II > I > III
GPF-IF/MDF-MTF	0.62 ± 0.05	0.61 ± 0.06	0.60 ± 0.06	0.498	
Rot-IOF/MDF-MTF	0.85 ± 0.06	0.85 ± 0.06	0.82 ± 0.07	0.163	

Values are presented as mean ± standard deviation.
FH, Frankfort horizontal plane.
See Table 2 for definition of each landmark.
*$p < 0.05$.
†Parameters used for correlation analysis with cephalometric parameters.

relatively stable during the growth period. Furthermore, the foramen is not an artificial but an anatomical structure. Since there was no sufficient information about parameters based on the foramina, the present study tried various parameters to analyze the different skeletal facial types and compared them to the conventional cephalometric parameters as a gold standard.

As shown in Tables 3 and 4, the three groups showed different maxillo-mandibular morphologies, even though the length of the anterior cranial base did not significantly differ between groups. Kasai et al.[25] reported no differences in the anterior cranial base lengths between Class I and Class II. As expected, the Class III group in the present study showed a shorter maxillary length, and the Class II group showed a shorter mandibular length. The Class II female group also showed a steeper mandibular plane angle. This downward and backward rotation of the mandible may reinforce the retrognathic mandible.[26,27] The Class III female group had a larger gonial angle than the other groups in the present study. The larger obtuse gonial angle would lead to a greater effect on the length of the mandibular body and ramus.[28] The results confirmed that the overall sample selection was well performed for the different facial skeletal types, especially in female patients.

The distance between Rot and Ov did not differ significantly between groups (Tables 5 and 6), which meant that the Rot and the Ov through which the maxillary nerve and the mandibular nerve exit from the cranium may be located in a similar position regardless of skeletal facial type. However, this result may have been because of the lack of differences in the cranial base length be-

Table 6. Comparison of foramina-based cone-beam computed tomography (CBCT) parameters in female patients in the three groups

CBCT parameter	Class I (n = 37)	Class II (n = 40)	Class III (n = 13)	Kruskal–Wallis	Mann–Whitney
Rot-Ov (mm)	16.2 ± 1.6	16.2 ± 1.6	16.0 ± 1.3	0.842	
Rot-IOF (mm)	46.5 ± 2.9	47.9 ± 3.4	47.6 ± 4.1	0.174	
Rot-GPF (mm)	34.4 ± 2.6	34.3 ± 3.0	32.8 ± 2.3	0.193	
Rot-IF (mm)†	62.6 ± 4.0	62.2 ± 4.0	58.7 ± 3.4	0.010*	I, II > III
GPF-IF (mm)	34.3 ± 2.5	35.1 ± 2.8	36.1 ± 2.8	0.105	
IOF-IF (mm)	38.1 ± 2.1	38.0 ± 2.3	36.4 ± 2.1	0.062	
Ov-MTF (mm)†	86.7 ± 4.5	83.3 ± 4.2	89.0 ± 4.7	< 0.001*	I, III > II
MDF-MTF (mm)†	54.0 ± 2.9	52.0 ± 3.0	55.9 ± 2.8	< 0.001*	I, III > II
Ov-MDF (mm)†	44.1 ± 3.5	41.9 ± 3.1	44.3 ± 3.1	0.008*	I, III > II
IOF-MTF (mm)†	65.9 ± 3.6	67.2 ± 4.5	65.5 ± 4.7	0.195	
IF-MTF (mm)†	44.7 ± 2.9	46.3 ± 3.8	45.9 ± 3.2	0.087	
Rot-IOF to FH plane (°)	15.5 ± 2.9	15.6 ± 3.3	15.8 ± 2.2	0.947	
Rot-GPF to FH plane (°)	63.7 ± 4.4	63.4 ± 3.4	64.4 ± 2.6	0.726	
GPF-IF to FH plane (°)†	16.2 ± 3.2	16.4 ± 3.8	14.9 ± 2.4	0.271	
IOF-IF to FH plane (°)	47.1 ± 2.7	46.6 ± 3.0	44.6 ± 2.7	0.030*	I > III
Ov-MDF to FH plane (°)	65.9 ± 2.7	66.9 ± 2.8	62.8 ± 2.7	< 0.001*	I, II > III
Ov-MTF to FH plane (°)	54.8 ± 3.2	58.5 ± 3.9	52.3 ± 2.9	< 0.001*	II > I > III
MDF-MTF to FH plane (°)†	34.5 ± 4.0	38.6 ± 5.4	33.8 ± 3.2	< 0.001*	II > I, III
Ov-MDF-MTF angle (°)†	124.1 ± 3.9	124.6 ± 4.2	124.9 ± 4.3	0.869	
Rot-GPF/Ov-MDF	0.78 ± 0.05	0.82 ± 0.07	0.74 ± 0.07	< 0.001*	II > I, III
Rot-IF/Ov-MTF	0.72 ± 0.03	0.75 ± 0.04	0.66 ± 0.03	< 0.001*	II > I > III
GPF-IF/MDF-MTF	0.64 ± 0.04	0.68 ± 0.07	0.65 ± 0.07	0.007*	I > II
Rot-IOF/MDF-MTF	0.86 ± 0.06	0.92 ± 0.08	0.86 ± 0.10	0.001*	I > II

Values are presented as mean ± standard deviation.
FH, Frankfort horizontal plane.
See Table 2 for definition of each landmark.
*$p < 0.05$.
†Parameters used for correlation analysis with cephalometric parameters.

tween groups. Thus, the outcomes might be different in patients with severe anomalies of the cranial base.

The maxillary nerve and its branches run through the Rot, IOF, GPF, and IF. Five linear and four angular parameters were defined from these foramina to evaluate significant differences among the Class I, Class II, and Class III malocclusion groups. There were no significant differences in the male patients in the three groups. However, two parameters, Rot-IF length and IOF-IF to FH plane angle, were significantly smaller in female patients in the Class III group than in the Class I and Class II groups (Table 6). The Class III female group in this study showed a slightly small (Co-A length, 86.1 mm) and retruded (SNA, 78.8°) maxilla, and there was high correlation between the Rot-IF length and the effective maxillary length (r = 0.707). Therefore, these findings indicate that the location of the IF is closely related to the size and position of the maxilla. In other words, patients with a retrognathic maxilla probably have further backward IF, and possibly *vice versa*.

The parameters using the foramina for the mandibular nerve showed more significant differences between groups in both genders. This study's results showed that the lengths of Ov-MTF, MDF-MTF, and Ov-MDF were significantly shorter in the Class II group than in the Class I and Class III groups. Shorter lengths from the Ov to the MTF may be attributable to the small and retrognathic mandible of Class II patients. This relationship

https://doi.org/10.4041/kjod.2019.49.5.326

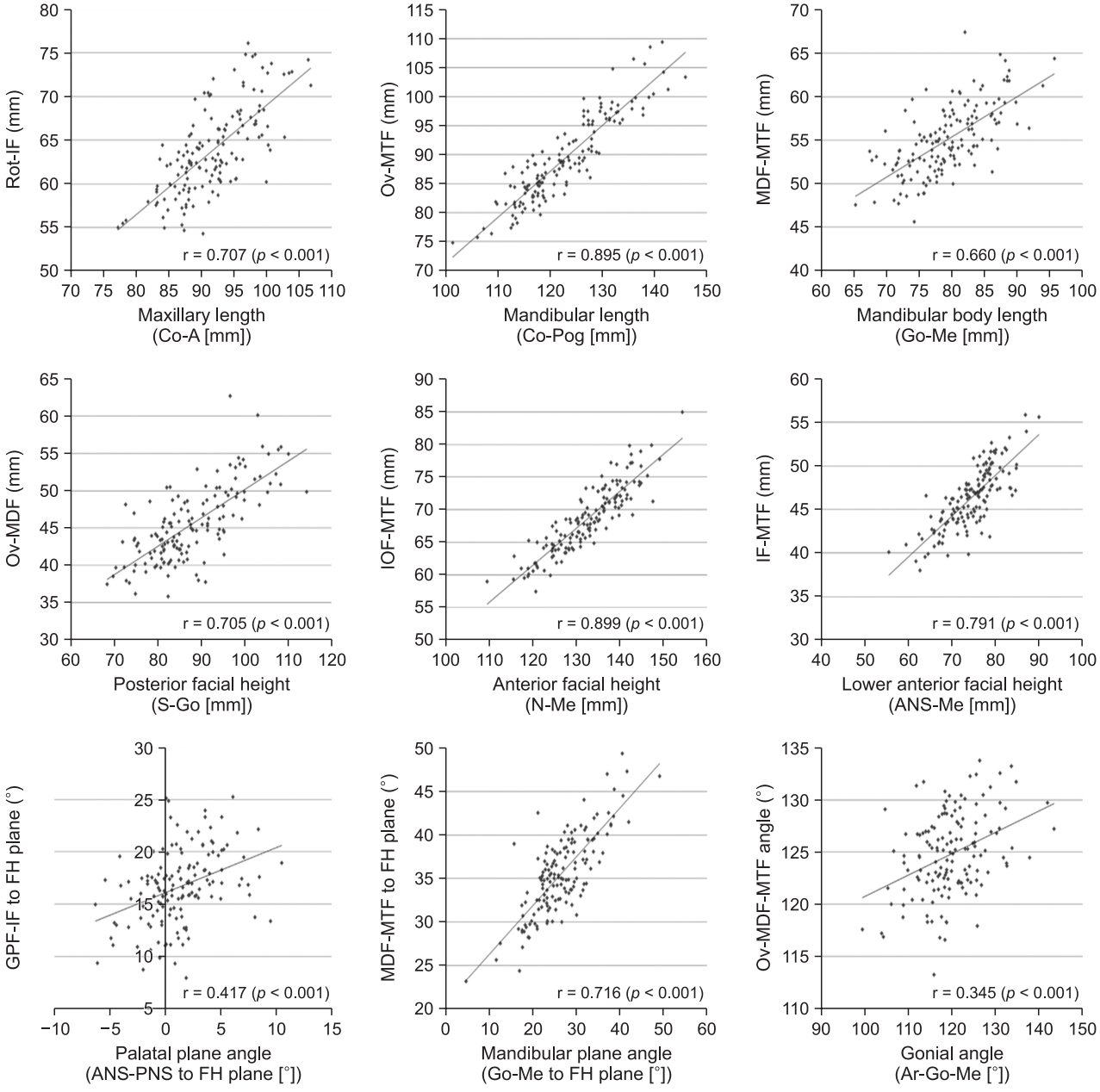

Figure 4. Spearman correlation analysis between conventional cephalometric parameters and the new cone-beam computed tomography parameters using foramina in maxillomandibular analysis.
See Tables 2 and 3 for definitions of each landmark or measurement.

was also established in the correlation analysis, which presented a high correlation (r = 0.895) between the Ov-MTF length and the mandibular length (Co-Pog). The planes of Ov-MDF and Ov-MTF showed greater obtuse angles to the FH plane in Class II than in Class III. These findings indicate that the MDF and the MTF are probably located further backward in Class II patients with a retrognathic mandible. The MDF-MTF to FH plane angle was greater in Class II than in the other groups, and because this parameter showed high correlation with the mandibular plane angle (r = 0.716), Class II patients with a high angle (hyperdivergence) may be expected to have a steeper mandibular canal. However, unlike other parameters, the Ov-MDF-MTF angle was not significantly larger in Class III than in the other groups, although the Class III female group showed a larger gonial angle. Correlation analysis also presented a relatively low correlation (r = 0.345) between these two parameters. This

 https://doi.org/10.4041/kjod.2019.49.5.326

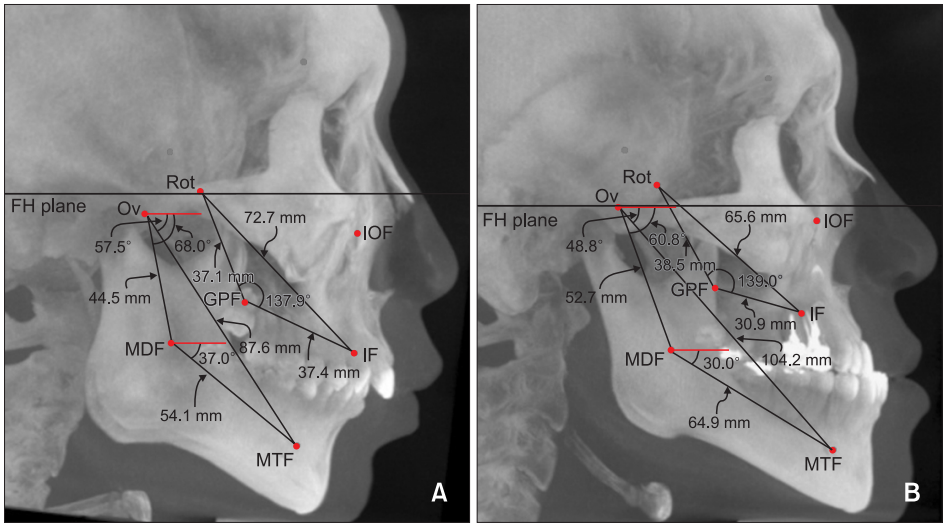

Figure 5. The locations of landmarks and measurements were visualized in the lateral maximum projection image of cone-beam computed tomography. Values of linear and angular parameters as measured in a 22-year-old male patient with skeletal Class II malocclusion **(A)**, and a 23-year-old male patient with skeletal Class III malocclusion **(B)**.
FH, Frankfort horizontal plane. See Table 2 for definition of each landmark.

mismatch between Ov-MDF-MTF angle and the mandibular shape represented by the gonial angle may be caused by superficial bone remodeling that may occur in the posterior region of the mandibular ramus due to the action of masticatory muscles.

Figure 5 shows representative examples of the skeletal Class II and Class III facial types. Notably, the IF and MTF are located at different positions depending on the skeletal morphology. With the results of this study we anticipate future application of new foramina-based parameters in analysis of skeletal malocclusion and in evaluation of the outcomes of orthopedic or surgical treatment. The present study examined only the parameters constructed by the landmarks itself, but additional 3D parameters constructed by projected points onto the three reference planes may be helpful for 3D analysis. The present study was conducted on adult patients, and studies on growing children may have yielded different results. Future studies will be required to identify longitudinal change patterns in these new parameters during the growth period and to compare them to the conventional cephalometric parameters. To date, cephalometric radiography has provided very useful data to establish treatment plans and evaluate treatment outcomes. Although the foramina-based parameters cannot replace 2D conventional cephalometric analysis in daily practice, these landmarks may be helpful in the research on the craniofacial growth and may be the key to early prediction of skeletal malocclusion. As mentioned by some previous researchers who used the foramina as landmarks for the evaluation of skeletal asymmetry,[9,29] these parameters using the nerve foramina may have the potential to be used for certain analysis, such as maxillary and/or mandibular asymmetry, transverse discrepancy, vertical discrepancy, and sagittal discrepancy as well.

CONCLUSION

The results of this study suggest that the foramina of the trigeminal nerve can be used for supplemental analysis in addition to conventional skeletal landmarks on the CBCT images.

CONFLICTS OF INTEREST

No potential conflict of interest relevant to this article was reported.

ACKNOWLEDGEMENTS

This study was supported by the 2015 research fund of Gangneung-Wonju National University (2015100204).

REFERENCES

1. Downs WB. The role of cephalometrics in orthodontic case analysis and diagnosis. Am J Orthod 1952;38:162-82.
2. Ricketts RM. Cephalometric synthesis: an exercise in stating objectives and planning treatment with tracings of the head roentgenogram. Am J Orthod 1960;46:647-73.
3. Ricketts RM. A foundation for cephalometric communication. Am J Orthod 1960;46:330-57.
4. Steiner CC. Cephalometrics for you and me. Am J Orthod 1953;39:729-55.
5. Steiner CC. Cephalometrics in clinical practice. Angle Orthod 1959;29:8-29.
6. Adams JW. Correction of error in cephalometric roentgenograms. Angle Orthod 1940;10:3-13.
7. Graber TM. Problems and limitations of cephalometric analysis in orthodontics. J Am Dent Assoc

1956;53:439-54.
8. Houston WJ. The analysis of errors in orthodontic measurements. Am J Orthod 1983;83:382-90.
9. Captier G, Lethuilier J, Oussaid M, Canovas F, Bonnel F. Neural symmetry and functional asymmetry of the mandible. Surg Radiol Anat 2006;28:379-86.
10. Kim SJ, Lee KJ, Lee SH, Baik HS. Morphologic relationship between the cranial base and the mandible in patients with facial asymmetry and mandibular prognathism. Am J Orthod Dentofacial Orthop 2013;144:330-40.
11. Lagravère MO, Gordon JM, Flores-Mir C, Carey J, Heo G, Major PW. Cranial base foramen location accuracy and reliability in cone-beam computerized tomography. Am J Orthod Dentofacial Orthop 2011;139:e203-10.
12. Ludlow JB, Laster WS, See M, Bailey LJ, Hershey HG. Accuracy of measurements of mandibular anatomy in cone beam computed tomography images. Oral Surg Oral Med Oral Pathol Oral Radiol Endod 2007;103:534-42.
13. Cutright B, Quillopa N, Schubert W. An anthropometric analysis of the key foramina for maxillofacial surgery. J Oral Maxillofac Surg 2003;61:354-7.
14. Scammon RE. The measurement of the body in childhood. In: Harris J, Jackson C, Paterson D, Scammon RE, eds. The measurement of man. Minneapolis: University of Minnesota; 1930.
15. Björk A. Prediction of mandibular growth rotation. Am J Orthod 1969;55:585-99.
16. Gudmundsson K, Rhoton AL Jr, Rushton JG. Detailed anatomy of the intracranial portion of the trigeminal nerve. J Neurosurg 1971;35:592-600.
17. Gray H, Warwick R, Williams PL. Gray's anatomy. 35th ed. London: Longman; 1973.
18. Dahlberg G. Statistical methods for medical and biological students. New York: Interscience Publications; 1940.
19. Behrents RG, Johnston LE Jr. The influence of the trigeminal nerve on facial growth and development. Am J Orthod 1984;85:199-206.
20. Gardner DE, Luschei ES, Joondeph DR. Alterations in the facial skeleton of the guinea pig following a lesion of the trigeminal motor nucleus. Am J Orthod 1980;78:66-80.
21. Moss ML. Neurotrophic processes in orofacial growth. J Dent Res 1971;50:1492-4.
22. Moss ML. An introduction to the neurobiology of oro-facial growth. Acta Biotheor 1972;21:236-59.
23. Pimenidis MZ, Gianelly AA. Class III malocclusion produced by oral facial sensory deprivation in the rat. Am J Orthod 1977;71:94-102.
24. Sarnat BG, Feigenbaum JA, Krogman WM. Adult monkey coronoid process after resection of trigeminal nerve motor root. Am J Anat 1977;150:129-37.
25. Kasai K, Moro T, Kanazawa E, Iwasawa T. Relationship between cranial base and maxillofacial morphology. Eur J Orthod 1995;17:403-10.
26. Sassouni V. A classification of skeletal facial types. Am J Orthod 1969;55:109-23.
27. Schudy FF. Vertical growth versus anteroposterior growth as related to function and treatment. Angle Orthod 1964;34:75-93.
28. Sanborn RT. Differences between the facial skeletal patterns of Class III malocclusion and normal occlusion. Angle Orthod 1955;25:208-22.
29. Minich CM, Araújo EA, Behrents RG, Buschang PH, Tanaka OM, Kim KB. Evaluation of skeletal and dental asymmetries in Angle Class II subdivision malocclusions with cone-beam computed tomography. Am J Orthod Dentofacial Orthop 2013;144:57-66.